



Enlisting a Traditional Chinese Medicine to tune the gelation kinetics of a bioactive tissue adhesive for fast hemostasis or minimally invasive therapy

Haoqi Tan^a, Dawei Jin^b, Junjie Sun^a, Jialin Song^a, Yao Lu^a, Meng Yin^b, Xin Chen^a, Xue Qu^{a,*}, Changsheng Liu^{a,**}

^a Key Laboratory for Ultrafine Materials of Ministry of Education, Frontiers Science Center for Materiobiology and Dynamic Chemistry, School of Material Science and Engineering, East China University of Science and Technology, Shanghai, 200237, China

^b Department of Cardiothoracic Surgery, Shanghai Children's Medical Center, School of Medicine, Shanghai Jiao Tong University, 1678 Dong Fang Road, Shanghai, 200127, China

ARTICLE INFO

Keywords:

Injectable tissue adhesive
Gelation time
Borax
Rapid hemostasis
Minimally invasive delivery

ABSTRACT

Gelation kinetics is important in tailoring chemically crosslinked hydrogel-based injectable adhesives for different applications. However, the regulation of gelation rate is usually limited to varying the gel precursor and/or crosslinker concentration, which cannot reach a fine level and inevitably alters the physical properties of hydrogels. Amidation reactions are widely used to synthesize hydrogel adhesives. In this work, we propose a traditional Chinese medicine (Borax)-input strategy to tune the gelation rate of amidation reaction triggered systems. Borax provides an initial basic buffer environment to promote the deprotonation process of amino groups and accelerate this reaction. By using a tissue adhesive model PEG-lysozyme (PEG-LZM), the gelation time can be modulated from seconds to minutes with varying Borax concentrations, while the physical properties remain constant. Moreover, the antibacterial ability can be improved due to the bioactivity of Borax. The hydrogel precursors can be regulated to solidify instantly to close the bleeding wound at emergency. Meanwhile, they can also be customized to match the flowing time in the catheter, thereby facilitating minimally invasive tissue sealing. Because this method is easily operated, we envision Borax adjusted amidation-type hydrogel has a promising prospect in clinical application.

1. Introduction

Injectable adhesives, based on two-component cross-linking in situ, are widely used in clinic due to their convenient delivery and high shape adaptability [1–3]. Amidation reaction triggered injectable hydrogels are superior to other chemically crosslinked hydrogels in terms of their inherent covalent binding ability towards biological tissue interface, as thus are currently being explored for tissue adhesives [4–7]. As we previously reported, an injectable polyethylene glycol-Lysozyme (PEG-LZM) hydrogel adhesive was developed for wound closure and tissue repair through the amidation reaction between the 4-arm-PEG-NHS (succinimidyl carbonate) and the amine groups on LZM [8]. The gelation time of this hydrogel, similar to other commercially available PEG adhesives, for instance DuraSeal™ or CoSeal® adhesive, is usually about tens of seconds to minutes in the phosphate buffer at pH 7.4 [9].

As an important parameter of injectable hydrogel, gelation rate largely determines the applicable scenario of the gel [10–15]. For hemostasis purposes, hydrogels should form rapidly after injection in order to prevent wound bleeding in time [16,17]. For certain deep wound sealing applications, slow and controlled gelation would be desirable to fill in irregularly shaped defects prior to solidification [18,19]. Moreover, for treating closed wounds such as gastric perforation [20,21], lung rupture [22,23], and liver injury [24,25], etc., the delivery of hydrogel precursor fluids in a minimally invasive and time-controlled manner before accessing the wound site is highly required [26].

However, the relatively fixed gelation rate makes it technically challenging when using such hydrogels for customized wound treatment [27–30]. Usually, the control of the gelation rate of most injectable chemically crosslinked systems is limited to varying the gelling precursor and/or crosslinker concentration, which cannot regulate gelation rate subtly, and inevitably changes their physical properties for instance

* Corresponding author.

** Corresponding author.

E-mail addresses: quxue@ecust.edu.cn (X. Qu), liucs@ecust.edu.cn (C. Liu).

<https://doi.org/10.1016/j.bioactmat.2020.10.011>

Received 8 August 2020; Received in revised form 8 October 2020; Accepted 19 October 2020

2452-199X/© 2020 The Authors. Production and hosting by Elsevier B.V. on behalf of KeAi Communications Co., Ltd. This is an open access article under the CC

BY-NC-ND license (<http://creativecommons.org/licenses/by-nc-nd/4.0/>).

mechanical strength, inner structure, degradation speed and so on [31–36]. There is a growing demand for developing a simple and efficient strategy to precisely regulate the gelation time with little or no alteration to the material's other properties.

Theoretically, the amidation reaction proceeds via the attack of nucleophilic N atom towards the electron-deficient acyl C atom [37]. The one-pair electron on N, once being protonated, will greatly reduce the nucleophilicity of N, and prevent the amidation reaction from occurring [38–41]. Therefore, how to promote the N deprotonation process is critical to accelerate the reaction rate. During the PEG-LZM crosslinking process, the protonation tendency of -NH_2 on LZM is influenced by the initial solution pH. We anticipate if a suitable chemical with a certain buffer capacity can alleviate the pH decrease during the reaction process, which can enhance the nucleophilicity of -NH_2 on the protein, as thus control the gelation time in a dose-dependent manner (i. e. shortened).

Borax, as a traditional Chinese medicine, has multiple bioactivities including antiseptic, antibacterial, antifungal, and antiviral, etc. [42, 43]. In clinic, borax is widely used for disinfection and antiseptic treatment of skin diseases [44]. While in chemistry, borax is a typical strong base-weak acid salt, and denoted as $\text{Na}_2\text{B}_4\text{O}_7 \cdot 10\text{H}_2\text{O}$. After dissolved in water, the boronic acid ion $\text{B}_4\text{O}_7^{2-}$ is hydrolyzed into equal quantities of boric acid $\text{B}(\text{OH})_3$ and tetrahydroxyborate ion $\text{B}(\text{OH})_4^-$, between which an acid-base equilibrium ($\text{p}K_a \approx 9.2$) is established with the capability to buffer the solution pH at a weak basic level [45–47].

Based on this, we hypothesize that the addition of borax could consume H^+ to promote the deprotonation of amino groups, and thus catalyze the amidation reaction between PEG and LZM. Secondly, the introduction of Borax into the hydrogel could provide additional bio-activities. Thirdly, as the byproduct (N-hydroxysuccinimide) ultimately induces a weak acidic environment in the gel matrix, the addition of Borax could retard pH decrease and make the pH of material similar to tissue. Scheme 1a illustrates that an injectable PEG-LZM adhesive system with customized gelation kinetics can be easily obtained by a simple Borax-input strategy. The amount of the initially added Borax precisely controls its gelation time ranging from seconds to minutes. Scheme 1b illustrates the potential applications of the hydrogel adhesive. Model 1 represents an emergent therapy case. The PEG-LZM/Borax (10 mg mL^{-1} Borax) can gelatinize within 3 s to instantly close the rabbit left ventricle wall defect and stop bleeding. Model 2 represents a minimally invasive

therapy case. The gelation time can be regulated to match the flow time of the hydrogel precursors in the catheter, which may be used for gastric perforation minimally invasive closure. In the meantime, the hydrogel also displays good antibacterial activities.

Our work reveals that the use of Borax confers the amidation-type hydrogel system with predetermined gelation time, therefore such adhesives can be customized for different therapy requests. Since Borax is a common clinical drug and the incorporation of Borax is operated easily, we envision Borax tuned amidation-type hydrogel has a promising prospect in clinical application.

2. Experimental section

2.1. Materials and tools

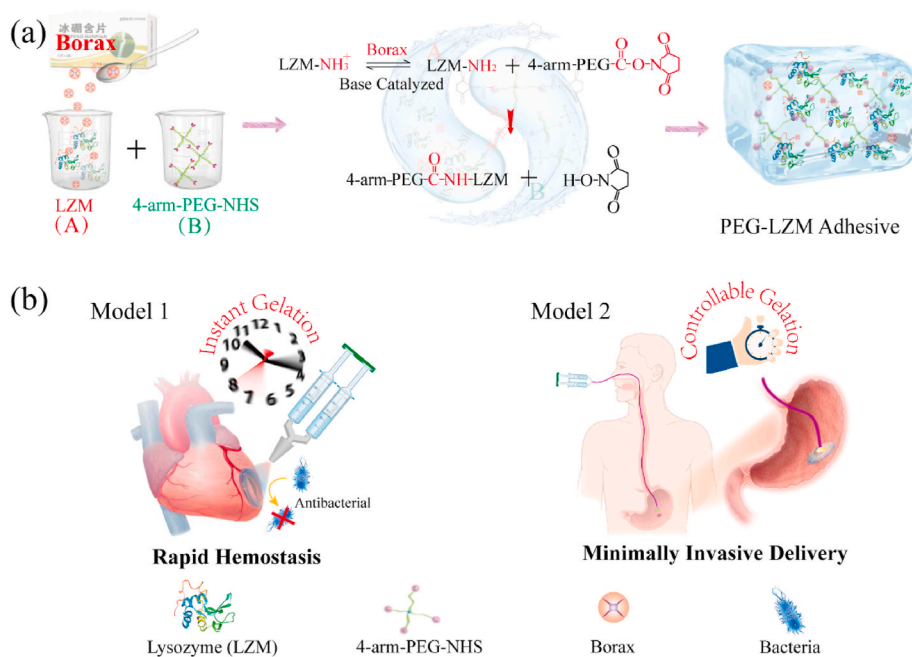
4-arm-poly (ethylene glycol) succinimidyl carbonate (4-arm-PEG-NHS (SC), $M_w = 10 \text{ kDa}$, $M_w/M_n = 1.03$) was purchased from SINOPEG, China. Sodium tetraborate decahydrate (Borax, AR) was purchased from Adamas-beta® co. LTD, China. All other materials or reagents were purchased from Sigma-Aldrich unless otherwise specified. Double cylinder syringe and spraying tip were purchased from Shanghai misawa medical industry co. LTD, China.

2.2. Hydrogel preparation

Before preparing hydrogel, the LZM protein was purified through a dialysis-lyophilization process (3 days), and then saline solution (0.9%, w/v) was firstly used to dissolve different contents of borax to prepare different concentrations of borax solution. Next, the prepared borax solution was used as the solvent to dissolve LZM (15%, w/v) as the precursor A. At the same time, the normal saline (0.9%, w/v) was used to dissolve 4-arm-PEG-NHS (15%, w/v) as the precursor B. Finally, the PEG-LZM/Borax hydrogels with different gelation time can be formed in situ after mixing the two components with a double cylinder syringe. (A: B = 1:1, v/v).

2.3. Measurement of gelation time

The gelation time was determined by the vial tilting method. Simply, according to the above method, prepared precursors were mixed and



Scheme 1. (a) The gelation time of PEG-LZM hydrogel can be regulated by a traditional Chinese medicine (Borax)-input strategy, which provides an initial basic buffer to promote the deprotonation process of amino groups and accelerate the amidation reaction. (b) For applications, Model 1 represents an emergent therapy case. The PEG-LZM with the fastest gelation time ($\leq 3 \text{ s}$) can instantly close the rabbit left ventricle wall defect and stop bleeding. Model 2 represents a minimally invasive therapy case. The gelation time can be regulated to match the flow time of the hydrogel precursors in the catheter, which pave the way for minimally invasive closure of deep tissue wound. Meanwhile, the improved antibacterial abilities of hydrogel can be achieved by Borax incorporation.

injected into a vial with a double cylinder syringe at room temperature (25 °C), and the time was regarded as the gelation time when there was no flow upon inverting the vial.

2.4. pH measurement

In this work, the pH of all solutions or hydrogels were measured with the microelectrode research system (PXF2078, Unisense, Denmark) containing micro-electrodes (tip diameter: 100 μm). Before each measurement, a process of calibration was performed to determine the corresponding relationship between the potential and the pH value, and then a standard curve was first generated automatically on the computer. Next, the clean pH working electrode and reference electrode were simultaneously inserted into the solution or gel (12 h after gelation), and then the pH of different samples was obtained based on the standard curve.

2.5. Ex vivo rapid sealing defect test

The defects (diameter: 2 mm) in pigskin or pig myocardium were first created by a punch, moreover, water was continuously injected into the myocardium defect through a catheter to simulate bleeding. In this experiment, 20 mg mL⁻¹ borax solution was used to dissolve LZM to achieve the rapid gelation speed of hydrogel. According to the above methods, 4 mL mixed precursors were quickly sprayed on the surface of pigskin or myocardium, and the results of gelation around defect was examined immediately after spraying or injecting.

2.6. Ex vivo simulated minimally invasive delivery study

In order to verify the feasibility of the hydrogel delivery by minimally invasive means, a catheter (NOGA MyoStar, 27 G, 30 cm) was connected to a double cylinder syringe, the other end was placed on the top of a 2 mL centrifuge tube. Then, normal saline was injected with a syringe pump through the catheter at a flow rate of 2 mL min⁻¹, and the flowing time of the normal saline in the catheter was recorded. Next, the gelation time of hydrogel was adjusted by borax content to match the recorded time. Finally, the prepared gelling solution was injected under the same conditions, and the gelation condition at the outlet of the catheter was recorded by camera.

2.7. Rheological study

In this experiment and next tissue adhesion study, different concentrations of borax solution (20, 12, 8, 4 mg mL⁻¹) was used to dissolve LZM to prepare hydrogel.

The PEG-LZM/Borax hydrogels were prepared as disc-shaped samples with a diameter of 20 mm. The viscoelastic behaviors of the hydrogels were measured by a Thermo Haake MARS rheometer. Before the tests, an amplitude sweep was first performed in order to define the linear viscoelastic region (LVR) in which the storage modulus is independent to the strain amplitude. Oscillation frequency sweep tests from 0 Hz to 10 Hz were selected to perform the rheological studies. The storage modulus G' represents the elastic property of the hydrogel, and the loss modulus G'' represents the viscous properties.

2.8. Lap shear adhesion strength test

Adhesive properties of hydrogels were determined by using lap shear adhesion test according to American Society for Testing and Materials (ASTM) standard F2255–05 [48]. The pigskin was washed by PBS and cut into small pieces (1 cm × 2.5 cm), then 200 μL mixed precursors were sprayed into the gap between the two pieces of pigskin and adhered them together. Then, the two pieces of pigskin were fixed between two glass sheets (5 cm × 2 cm) with rough surface by a cyanoacrylate glue (gold elephant 508). 60 min later, the glass sheets were

clamped by a universal mechanical tensile machine (SANS CMT2503) to stretch (tensile rate was set as 5 mm min⁻¹). The maximum stress during the stretching process was esteemed as the adhesive strength of the hydrogel for pigskin. (n = 4).

2.9. In vitro antimicrobial study

In the following experiments, different borax solution was used to dissolve LZM unless otherwise mentioned. *Staphylococcus aureus* (*S. aureus*, ATCC 25923) and methicillin-resistant *Staphylococcus aureus* (MRSA, acquired from the Second Affiliated Hospital of Zhejiang University) were chosen as the model of Gram-positive bacteria, and *Escherichia coli* (*E. coli*, ATCC 25922) was chosen as the model of Gram-negative bacteria. Firstly, 2 mL PEG-LZM (PEG and LZM were dissolved in 0.1 M PB) or PEG-LZM/Borax hydrogel was prepared in each well according to the above method. Then, 1 mL different bacterial suspension (10⁷ CFU mL⁻¹, 100% medium) was added to each well. After culturing at 37 °C for 12 h, the bacteria morphology was observed by surface morphology observation (SEM, 10 kV), and number of remaining viable bacteria in the suspension was measured by dilution plate counting (10³). (n = 3).

Next, to further demonstrate the enhanced antibacterial activity of PEG-LZM/Borax hydrogel, the anti-biofilm formation experiment was performed. In this study, 2 mL of MRSA fluid (10⁷ CFU mL⁻¹, 100% high sugar medium, 1% glucose) was added in each well for co-incubation with different samples at 37 °C for 48 h. After incubation, each sample was taken out and washed by saline for 5 times. The biofilm formation on the surface of each sample was characterized by SEM and live/dead bacterial fluorescent staining (1.67 mM SYTO 9 and 20 mM propidium iodide).

2.10. In vivo antimicrobial study

In vivo studies were performed in strict accordance with National Institutes of Health (NIH) guidelines for the care and use of laboratory animals (NIH Publication no. 85-23 Rev. 1985) and all procedures were approved by the Research Center for Laboratory Animals of Shanghai University of Traditional Chinese Medicine (Shanghai, China).

To evaluate the antibacterial properties of hydrogel in vivo, we created two skin wounds (diameter 10 mm) on the back of each rat, and contaminated them with 10 μL MRSA (10⁸ CFU/mL) fluid, respectively. 200 μL cooled mixture of PEG-LZM/Borax hydrogel (10 mg mL⁻¹ Borax) precursor was injected in the right wound, while the left wound treated with 3 M dressing served as control. For statistical analysis, 5 rats were used for this study. 3 days after operation, the animals were euthanized by inhaling an anesthetic and the wounds were photographed by camera. The bacteria at the wound site were collected by cotton swab for diluted plate assay and then the skin of the wounds was excised for H&E staining.

2.11. In vitro compatibility study

2.11.1. Cell culture

To study the cell affinity of the PEG-LZM/Borax hydrogel, murine myoblast cells (C2C12) and murine-derived L929 fibroblast cells purchased from the American Type Culture Collection (ATCC, VA, USA) were used for evaluating the cytotoxicity of hydrogels. The Cell culture and cell implantation are presented in supplementary information.

2.11.2. Cell attachment studies

According the above method, 500 μL mixed hydrogel precursors (10 mg mL⁻¹ Borax) was prepared in the each well of a 24 well plate. Then, C2C12 cells and L929 cells were seeded on the surface of the hydrogels or cell plate at a density of 3 × 10⁴ cells per well with 12 h incubation.

Next, immunofluorescent staining was performed after cells were fixed in 2.5% glutaraldehyde solution for 15 min and permeabilized by

Triton X-100 (0.1%, v/v) for 10 min. Simply, samples were attained by PBS with $5 \mu\text{g mL}^{-1}$ of FITC (fluorescein isothiocyanate)-phalloidin (15 min) and $5 \mu\text{g mL}^{-1}$ of DAPI (4',6-diamidino-2-phenylindole) (15 min) for cytoskeleton and nuclei staining, respectively. The stained cells were observed by confocal laser scanning microscopy (CLSM, Nikon, Japan). Cell average spreading area was evaluated by randomly photographing cells on ten places of different samples and calculated using Image J software.

2.11.3. Cell proliferation studies

The cytocompatibility of the PEG-LZM/Borax hydrogel was evaluated by Cell Counting Kit-8 (CCK-8, Dojindo, Japan) and Live/Dead fluorescent staining. For this study, C2C12 cells and L929 cells were seeded onto the hydrogel surface. For cell proliferation analysis, the medium containing 2% fetal bovine serum (FBS) was replaced by fresh medium containing 10% CCK-8 after culture for 1, 3, and 5 days. The incubation solution was then transferred to a 96-well plate after 2 h of incubation and the absorbance was measured using a microplate reader at 450 nm (Model 550, Bio-Rad, USA). For live/dead assay, the each well was washed with PBS for 3 times, and then the cells were stained with calcein AM and propidium iodide according to the kit instruction (Thermo Fisher, L3224), and then imaged by inverted fluorescence microscope (Leica, DMI3000B).

2.11.4. Hemolytic properties study

The hemolytic properties of PEG-LZM/Borax hydrogel was estimated. Simply, fresh blood of rabbit was centrifuged at 1200 g for 15 min to remove the upper serum. The obtained plasma was washed with PBS buffer (repeated 3 times), then 1 mL rabbit blood cells (40%, v/v) in PBS buffer (pH 7.4) was incubated with hydrogel (500 μL) for 1 h at 37 °C. At the same time, 500 μL PBS buffer or 0.1% Triton X-100 solution was added into rabbit blood cells suspension as positive and negative controls, respectively. These tubes were then centrifuged at 1200 g for 15 min and absorbance at 540 nm of supernatant was measured by a microplate reader (SpectraMaxi, Molecular Devices). The ratio of hemolysis for PEG-LZM/Borax hydrogel was calculated as:

$$\text{Hemolysis (\%)} = \frac{A_h - A_p}{A_t - A_p} \times 100\%$$

Where A_h , A_p and A_t represent absorbance of hydrogels group, positive group (PBS) and negative group (Triton X), respectively. (n = 3).

2.12. In vivo biocompatibility study

100 μL cooled mixture of PEG-LZM/Borax hydrogel (10 mg mL^{-1} Borax) precursors was injected into the dorsal subcutaneous pocket (between skin and muscle) of Sprague Dawley (SD) rats (200–300 g). The rats were sacrificed after 1 week. The samples and surrounding tissues were fixed, sectioned, embedded, and stained with hematoxylin and eosin (H&E). (n = 3).

2.13. Rapid closure of transmural left ventricular (LV) wall defect to stop bleeding

New Zealand white rabbits were used as the animal model in this study. The rabbit was first anesthetized by ear vein injection with 40–50 mg kg^{-1} pentobarbital. Preoperative echocardiography measurements (ECHOs) were used to record the Left ventricular function (LVF) of each rabbit. Next, the preparatory works were finished in advance, such as tracheal intubation, breathing support, inhalation anesthesia, and nutritional fluid supply through the vein, etc. Then, the left ventricular (LV) was exposed after opening the chest, a transmural LV wall defect was created with a needle (inner diameter: 1.2 mm). The defect was immediately closed by injecting mixed precursors of PEG-LZM/Borax (10 mg mL^{-1} Borax), and then situation of heart beats and defect

closure were examined immediately. Finally, the chest of rabbits was closed according to conventional cardiothoracic surgery clinical surgical operation. After 2 days and 3 weeks postoperatively, the left ventricular systolic function of rabbits was examined by ECHOs respectively, and the wound recovery was observed by Masson's trichrome staining (3 weeks). (n = 4).

2.14. Evaluation of gastric perforation sealing

Firstly, each rat was anesthetized by intraperitoneal injection with 0.8 mL of 1% w/v pentobarbital solution. Then, 20 mL of sterile normal saline was injected into abdominal cavity to clean the stomach, and then the normal saline was recycled for Rivalta assay and the analysis of nuclear cell number. Next, after exposing the rat's stomach, a 2 mm diameter defect was created. The defect was sealed by injecting mixed precursors of PEG-LZM/Borax (5 mg mL^{-1} Borax) through a suitable length of tube. Non-treatment and the defect treated by suturing were set as negative or positive control group, respectively.

The gastric wounds of rats were observed and recorded after 3 days and 2 weeks. After 2 weeks, washing fluid (normal saline) of abdominal cavity was collected again for Rivalta assay and the analysis of nuclear cell number according the above method. At last, the wound surrounding tissues were fixed with paraformaldehyde for sectioning, staining (H&E), and histological observation. (n = 4).

2.15. In vivo wound healing tests

Male Sprague Dawley (SD) rats (200–300 g) were selected for this study and the rats were randomly divided into 3 groups containing 4 replicate samples: (1) PEG-LZM/Borax; (2) PEG-LZM; (3) Control. Two wounds were created on the back of each rat with 10 mm in diameter, and then different types of hydrogels were injected to fill the wounds, while no treatment was applied to the control group. Finally, the rats were wrapped with medical gauze and fixed with adhesive tape. The wounds were photographed by digital camera at the predetermined time after surgery.

2.16. Statistical analysis

All data were expressed with mean standard deviation (SD) and analyzed using one-way ANOVA with post hoc tests. Significance was set at $p < 0.05$ (** $p < 0.001$, ** $p < 0.01$, * $p < 0.05$), while $p > 0.05$ was considered to be statistically nonsignificant (N.S.).

Other Experimental details are provided in the Supporting Information.

3. Results and discussion

3.1. Borax catalyzes the amidation reaction by its pH buffering ability

Fig. 1(a) displays the mechanism of the amidation reaction between protein and 4-arm-PEG-NHS, where the $-\text{NH}_2$ in protein (e.g. LZM) experiences a deprotonation step first, and then nucleophilically substitutes the $-\text{NHS}$ group at the end of 4-arm-PEG-NHS, forming a stable amido bond and assembling the polymeric network [8]. Since the protonation of $-\text{NH}_2$ is influenced by the initial pH as well as the acidic by-product (N-hydroxysuccinimide) during gelation, we expect a basic gelling environment can promote the N deprotonation process and catalyze the amidation reaction. We initiate an electrochemical test as indicated by Fig. 1(b) to confirm the speculation. Experimentally, an electrolyte was first prepared by dissolving the LZM and 4-arm-PEG-NHS into the normal saline with an acid-base indicator. A two-electrode system employing a Ti plate as the cathode and a Pt wire as the anode was set into the solution. Before imposing a potential, the electrolyte solution shows a yellow color (acidity) and no gelation was observed, indicating an acidic environment unfavored the gelation reaction. In contrast, a

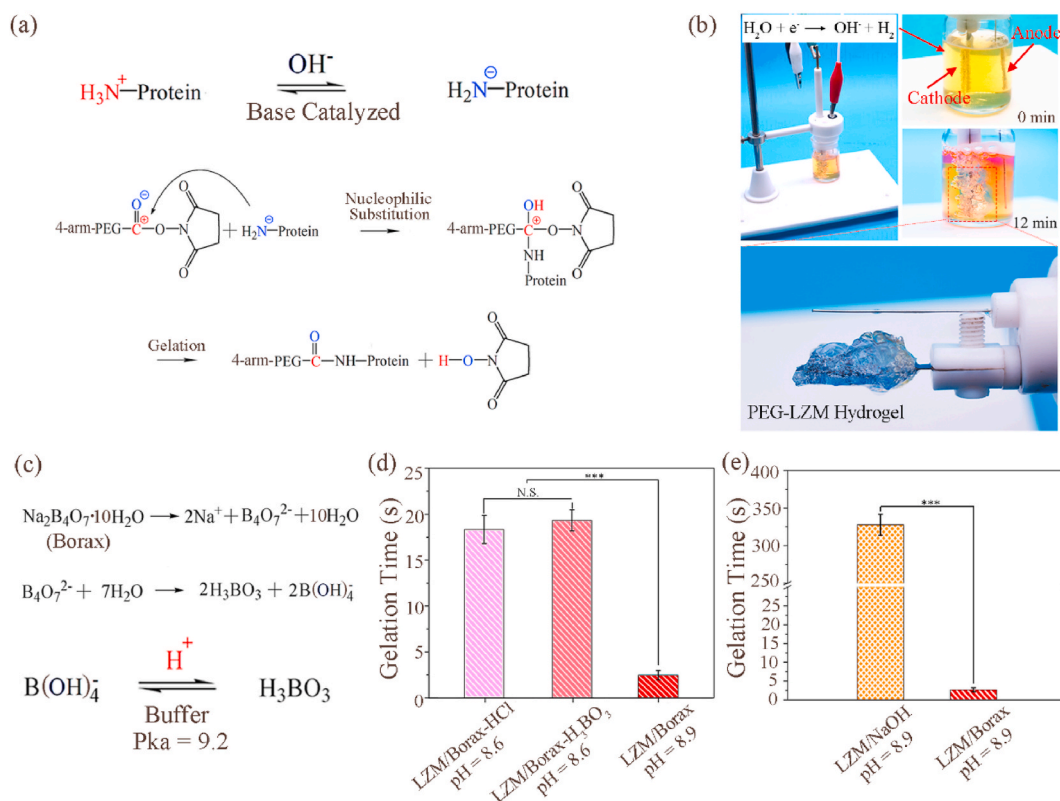


Fig. 1. Mechanism study of Borax regulating gelation rate. (a) The amidation reaction between protein and 4-arm-PEG-NHS; deprotonated $-\text{NH}_2$ attacks the electron-deficient C atom in the end of 4-arm-PEG-NHS to form PEG-LZM hydrogel and acidic by-product N-Hydroxysuccinimide (NHS). (b) Due to the effect of electrolyzed water, a large amount of OH^- was generated near the cathode and promote gelation reaction. (c) Borax can be hydrolyzed to provide equal quantities of boric acid ($\text{B}(\text{OH})_3$) and tetrahydroxyborate ion ($\text{B}(\text{OH})_4^-$), between which a buffer environment is established to consume protons (H^+). (d) Comparison of gelation time after adding boric acid (H_3BO_3) and hydrochloric acid (HCl) to precursor A. (e) The comparison of gelation time after the pH of precursor A was adjusted to the same level by using NaOH and Borax, respectively.

hydrogel formed rapidly on the cathodic Ti plate after powering up. Meanwhile, the solution near the cathode changed from yellow to blue (alkaline), which proved that a large amount of OH^- was generated from the water electrolysis and contributed to this fast gelation. Based on this, we can conclude that a basic gelling environment can catalyze the amidation gelation reaction.

Fig. 1(c) displays that Borax ionizes out Na^+ and $\text{B}_4\text{O}_7^{2-}$ in aqueous solution, of which $\text{B}_4\text{O}_7^{2-}$ further undergoes a hydrolysis reaction to provide equal quantities of boric acid $\text{B}(\text{OH})_3$ and tetrahydroxyborate ion $\text{B}(\text{OH})_4^-$, between which a buffer environment is established at a weak basic level to consume the existing protons (H^+) [45–47]. To confirm this, we put a certain amount of Borax into H_2O , LZM/ H_2O and 4-arm-PEG-NHS/ H_2O solutions respectively (Borax 20 mg mL^{-1}), and measured their pH variations. Fig. S1 shows that the addition of Borax can switched LZM/ H_2O and 4-arm-PEG-NHS/ H_2O solutions from weak acid to weak basic. We added Borax to the LZM solution (20 mg mL^{-1} Borax in precursor A; pH 8.9) and then mixed it with 4-arm-PEG-NHS water solution (precursor B). Fig. 1(d) indicates that a fast gelation within 3 s was observed in the presence of Borax. In contrast, two types of acids including H_3BO_3 and HCl were respectively used to reduce the pH of LZM/borax (precursor A) from 8.9 to the same 8.6. Their gelation time was both extended to the same degree. Therefore, these data demonstrate that the Borax promoted gelation process can be ascribed to its initial pH tuning ability instead of its elemental composition.

Next, in order to further confirm that borax solution can provide a certain buffer capacity to alleviate pH decrease for gelation, we used a non-buffered NaOH adjusted LZM solution at pH 8.9 to perform the same gelation reaction. As shown in Fig. 1(e), although the initial reactivity of $-\text{NH}_2$, which is determined by the initial pH, was the same

in both LZM/Borax and LZM/NaOH precursor, the LZM/Borax precursor once exposing to 4-arm-PEG-NHS, exhibited a much faster gelation rate. This is because the Borax with a strong buffering capacity can continuously improve $-\text{NH}_2$ deprotonation by “sucking” H^+ , which is evidenced by the decreased acidification of the resultant hydrogel due to Borax addition in Fig. S2.

Finally, to verify this Borax-input strategy can provide a generic means to control other amidation reactions, we replaced the LZM component with bovine serum albumin (BSA), human hemoglobin (HGB), and albumin (OVA), etc., and measured their reaction speed with 4-arm-PEG-NHS. As shown in Fig. S3(a), all of proteins presented poor reactivity with 4-arm-PEG-NHS in normal saline (no gelation occurred within 10 min), and all the mixed gelling solution was acidic after reaction (pH 3.1–3.6). In contrast, the gelation rate of all systems was obviously accelerated after borax adding, and all kinds of hydrogels could be formed quickly within 30 s. The final pH value of these hydrogels was between 6.0 and 6.5 (Fig. S3(b)). All these results demonstrate that Borax-input method provides a generic opportunity to regulate the reaction rate between protein and 4-arm-PEG-NHS through a simple pH controlling way.

3.2. Borax precisely regulates the gelation time in a dose-dependent manner

Since Borax can promote amidation reaction by its pH tuning ability, we then investigate the pH of the precursor (i.e. LZM solution) with varying Borax contents. Fig. 2(a) shows the dependence of the LZM solution pH on Borax level. The addition of Borax contents from 1.5–8 mg mL^{-1} dramatically raised solution pH from 7.42 to 8.75 (precursor

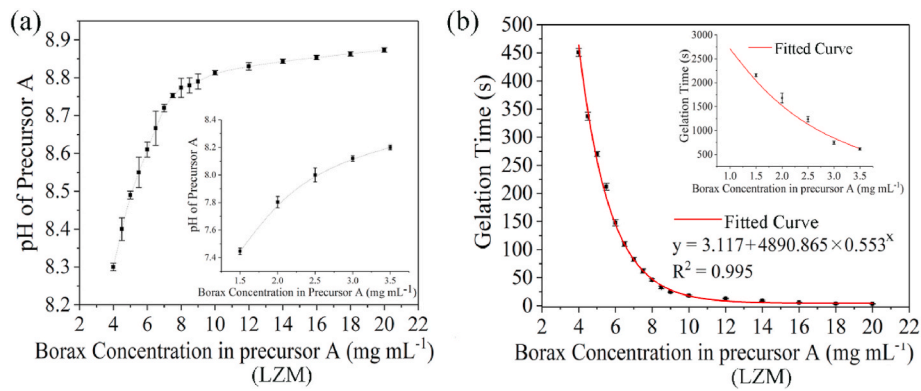


Fig. 2. (a) The pH of precursor A and (b) gelation time of the PEG-LZM/Borax hydrogel change with the various borax concentrations in precursor A. The inserts display the data measured at low Borax from 1.5–3.5 mg mL⁻¹. The gelation time with borax concentration follows an exponential equation.

A). While with more Borax over 8 mg mL⁻¹, the pH increase became more moderate.

The gelation time of hydrogels with different Borax contents from 1.5–20 mg mL⁻¹ is indicated in Fig. 2 (b). The insert displays the data at low Borax from 1.5–3.5 mg mL⁻¹. We observed a similar Borax influence on gelation time as shown in Fig. 2(b). The fitted curves of the relation between Borax concentration and gelation time were obtained, which fit

the experimental data very well ($R^2 = 0.995$). An exponential equation was also acquired and denoted as:

$$\text{Gelation Time (s)} = 3.117 + 4890.865 \times 0.553^{C_{\text{borax}}} \text{ (mg mL}^{-1}\text{)}$$

These results indicate the gelation time of the PEG-LZM hydrogel could be precisely controlled from seconds to minutes by different borax contents in precursor A, which can be mathematically predetermined.

In addition, as the byproduct (N-hydroxysuccinimide) in the



Fig. 3. Ex vivo modeling of customized gelation (a) The mixed gelling solution was sprayed evenly on (1) pigskin and (2) myocardium and solidify instantaneously to seal the model wounds even with gushing water. (b) Minimally invasive delivery of PEG-LZM/Borax hydrogel was simulated ex vivo, the mixed gelling solution flew smoothly in the minimally invasive catheter and solidified within a very short time at the outlet to seal the top of tube.

amidation reaction induces a weak acidic environment in the gel matrix, the addition of Borax could alleviate the pH decrease. Fig. S4 provides the evidence that the final pH of the resultant PEG-LZM hydrogels gradually increases to neutral with Borax increasing, which corresponds to the pH tuning ability of Borax.

3.3. Ex vivo modeling of gelation

3.3.1. Instant gelation for tissue closure

Most commercial adhesives are difficult to seal wound in the presence of body fluids due to their long gelation time. For example, the gelation time of PEG derivative-based DuraSeal™ and CoSeal® are respectively 1.0 min and 3.2 min, which are not suitable for emergent hemostasis [9]. In contrast, the PEG-LZM can be adjusted to gel within 3 s when using Borax at 20 mg mL⁻¹ in LZM precursor. As thus, such injectable hydrogel could be a good candidate for emergent tissue sealing.

Next, the two phase gel-forming precursor A/B were put into a double cylinder syringe (mixer) with an atomizing nozzle (Fig. S5). Through such a delivery tool, the two-phase precursor can be uniformly mixed in a very short time.

In order to verify its effect, we sprayed the gelling solution on the surface of the defective pigskin (Fig. 3(a)-1, Movie S1) and notched myocardium (Fig. 3(a)-2, Movie S2, bleeding was simulated by injecting water at the defect). The gelling solution was observed to be sprayed evenly on different surfaces and solidify instantaneously to seal the model wounds.

Supplementary video related to this article can be found at <https://doi.org/10.1016/j.bioactmat.2020.10.011>

3.3.2. Controlled gelation for minimally invasive tissue sealing

The difficult-to-adjust gelation time often sets a barrier for minimally invasive delivering injectable hydrogels for closed wounds sealing. For example, if the gelation time is too short, the delivery catheter or needle tube will be blocked, while overlong gelation time may cause delayed gelation and unsuccessful wound sealing [49]. Thus, we believe that the precisely controllable gelation of PEG-LZM by Borax can bring great convenience to clinical operation. A simulated minimally invasive delivery process was performed ex vivo. As illustrated in Fig. 3(b), a catheter (NOGA MyoStar, 27 G, 30 cm) was immersed into a water bath at 37 °C. It's one end was connected to a double cylinder syringe, and the other end was placed on the top of a 2 mL centrifuge tube. Then, a gelling solution supplemented with a predetermined Borax content that can modulate the gelation time consistent with the flow time of the hydrogel precursors in the catheter. Movie S3 clearly indicates the mixed gelling solution flew smoothly in the minimally invasive catheter and solidified within a very short time at the outlet to seal the top of

tube.

Supplementary data related to this article can be found at <https://doi.org/10.1016/j.bioactmat.2020.10.011>.

These ex vivo results demonstrate that PEG-LZM hydrogel can provide a variable gelation dynamic for customized wound treatment just by adjusting the incorporated Borax content.

3.4. The physical properties of hydrogel keep constant after borax addition

We investigated the influence of gelation rate on the mechanical properties and the adhesive strength of the hydrogels. The hydrogels containing 10, 6, 4, 2 mg mL⁻¹ borax were selected for these studies (20, 12, 8, 4 mg mL⁻¹ borax solution were selected to dissolve LZM as the precursor A), and their corresponding gelation time is about 3 s, 18 s, 142 s and 450 s, respectively.

The viscoelastic properties of PEG-LZM/Borax hydrogels were first studied. As shown in Fig. 4(a), no obvious difference of modulus (G' or G'') was observed among these hydrogels, indicating the viscoelastic properties and shear modulus of hydrogel were not obviously influenced by the change of gelation time.

Due to the remaining active groups on the 4-arm-PEG-NHS during gelation, the hydrogel can adhere to different tissues by forming amide bonds with abundant amino groups on tissue surface [4,6]. In order to investigate the influence of gelation rate on the tissue adhesive capacity, especially in the case of rapid gelation (within 3 s), two pieces of pigskin were adhered together by injecting the PEG-LZM/Borax gelling solution, and then the adhesion strength for pig skin was measured by stretching. As shown in Fig. 4(b), the adhesive strength of PEG-LZM/Borax hydrogels is about 20 kPa regardless of their gelation time, and has exceeded that of the fibrin glue (BeiXiu™, 14 kPa).

These results indicate that the physical properties of the PEG-LZM hydrogel remain constant even its gelation kinetics is altered. It is worth noting that, in the case of instant gelation, the use of a double-barrel syringe with a special nozzle is important for achieving a mechanically robust hydrogel, because it can mix the gelling solution uniformly in a very short time.

3.5. Borax addition improves the antibacterial activity of hydrogel

Borax, as a traditional Chinese medicine, is usually used to treat ulcerative or infected wounds. It is mainly involved in destroying the quorum-sensing of bacteria [50–52], and thus has obvious antibacterial activity. The antibacterial performance of PEG-LZM/Borax hydrogels were evaluated. To understand the contribution of borax to antibacterial activity, the pristine PEG-LZM hydrogel was used as a negative control. Both Gram-positive and Gram-negative bacteria were incubated in the

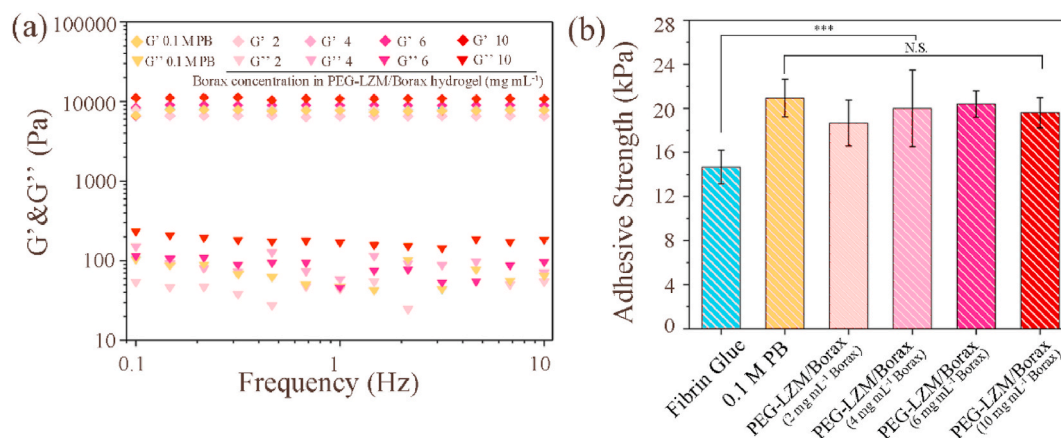


Fig. 4. Mechanical properties of PEG-LZM hydrogels with different Borax contents. (a) Rheological test, (b) adhesive strength of hydrogel test to pig skin.

presence of materials. The results in Fig. 5(a) and Fig. 5(b) show that the bacterial suspension exposed to PEG-LZM/Borax hydrogel generated less bacterial colonies on the plates, and the antibacterial ability became stronger with the increase of Borax content. The morphologies of bacteria with or without hydrogel contacting were examined by SEM. As shown in Fig. S6, the original shape of *E. coli* was rod-like, and *S. aureus* had a spherical shape. Because Borax and LZM can touch and destroy bacterial membrane, the severe destruction was found on the cell membranes that were treated with PEG-LZM/Borax hydrogel.

In order to further prove the improvement of antibacterial ability after the addition of borax, the PEG-LZM/Borax (10 mg mL⁻¹ Borax) hydrogel was used to challenge the resistance of MRSA biofilm formation in nutrient-rich medium (TSB medium supplemented with 1% glucose) for 48 h. Live/dead bacterial fluorescence staining assay was involved to stain the biofilm, as observed in Fig. 5(c), a layer of green fluorescence was observed on the surface of control group, indicating an MRSA biofilm was formed on PEG-LZM surface due to its weak antibacterial ability. In contrast, no biofilm was formed on PEG-LZM/Borax

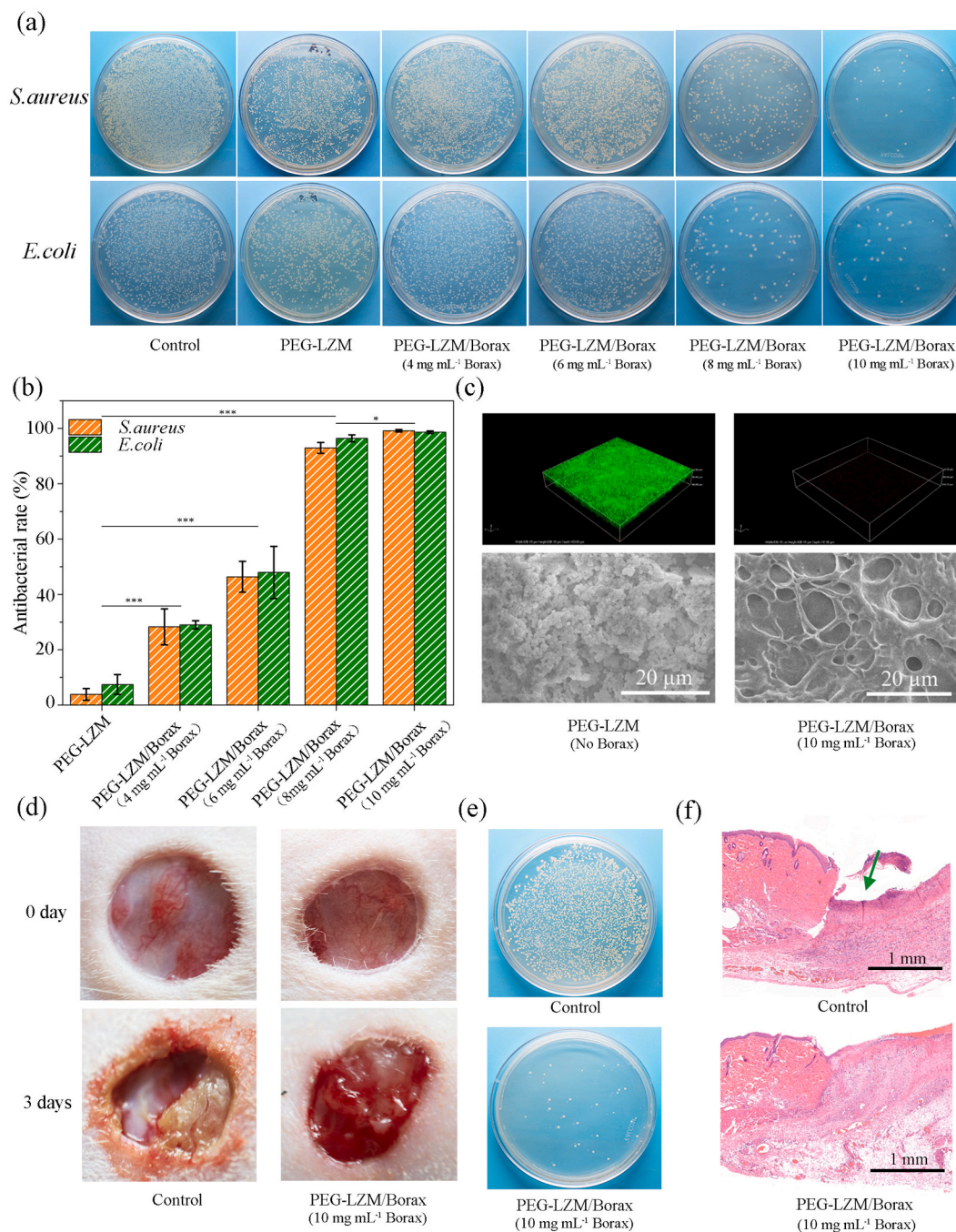


Fig. 5. Evaluation of antibacterial activity of PEG-LZM/Borax hydrogel. (a) Photographs of bacterial colonies formed by *S. aureus* and *E. coli* after exposing to PEG-LZM or PEG-LZM/Borax hydrogel, respectively. (b) The antibacterial rate of different samples. (c) Photographs of Live/Dead fluorescent staining and the SEM observation of MRSA biofilm on the surfaces of different samples. (d) In vivo antimicrobial studies. Photographs of wounds treated with commercial 3 M dressing or PEG-LZM/Borax hydrogel. (e) The bacteria were collected from the wound area and cultured on agarose gel media. (f) Histological analysis of surrounding wounds by H&E staining. (The green arrow indicates severe inflammatory cell infiltration). (For interpretation of the references to color in this figure legend, the reader is referred to the Web version of this article.)

hydrogel, because no green fluorescence was observed (the remaining bacteria have been easily washed away). SEM observations were consistent with these results, which revealed a well-formed MRSA biofilm on the PEG-LZM surface, while no biofilm structure on the PEG-LZM/Borax surface. These data prove that the better bacterial inhibition ability of hydrogel can be acquired due to the presence of borax.

Next, we further evaluated the antibacterial properties of PEG-LZM/Borax hydrogel in vivo, the defects of rat skin were contaminated with MRSA firstly and then PEG-LZM/Borax (10 mg mL^{-1} Borax) hydrogel

precursor was injected into the wound site. Fig. 5(d) shows the wound situations 3 days postoperatively. The control group treated with 3 M commercial dressing without antibacterial ability shows obvious suppurations due to serious bacterial infection. However, the wound area treated with PEG-LZM/Borax hydrogel has less (or no) inflammation. Bacteria in the wound area were collected for quantification by plate counting. As shown in Fig. 5(e), PEG-LZM/Borax resulted in an obvious decrease in number of bacteria in comparison with the control (average 1.9-Log reduction of bacterial number). Fig. 5(f) shows histological

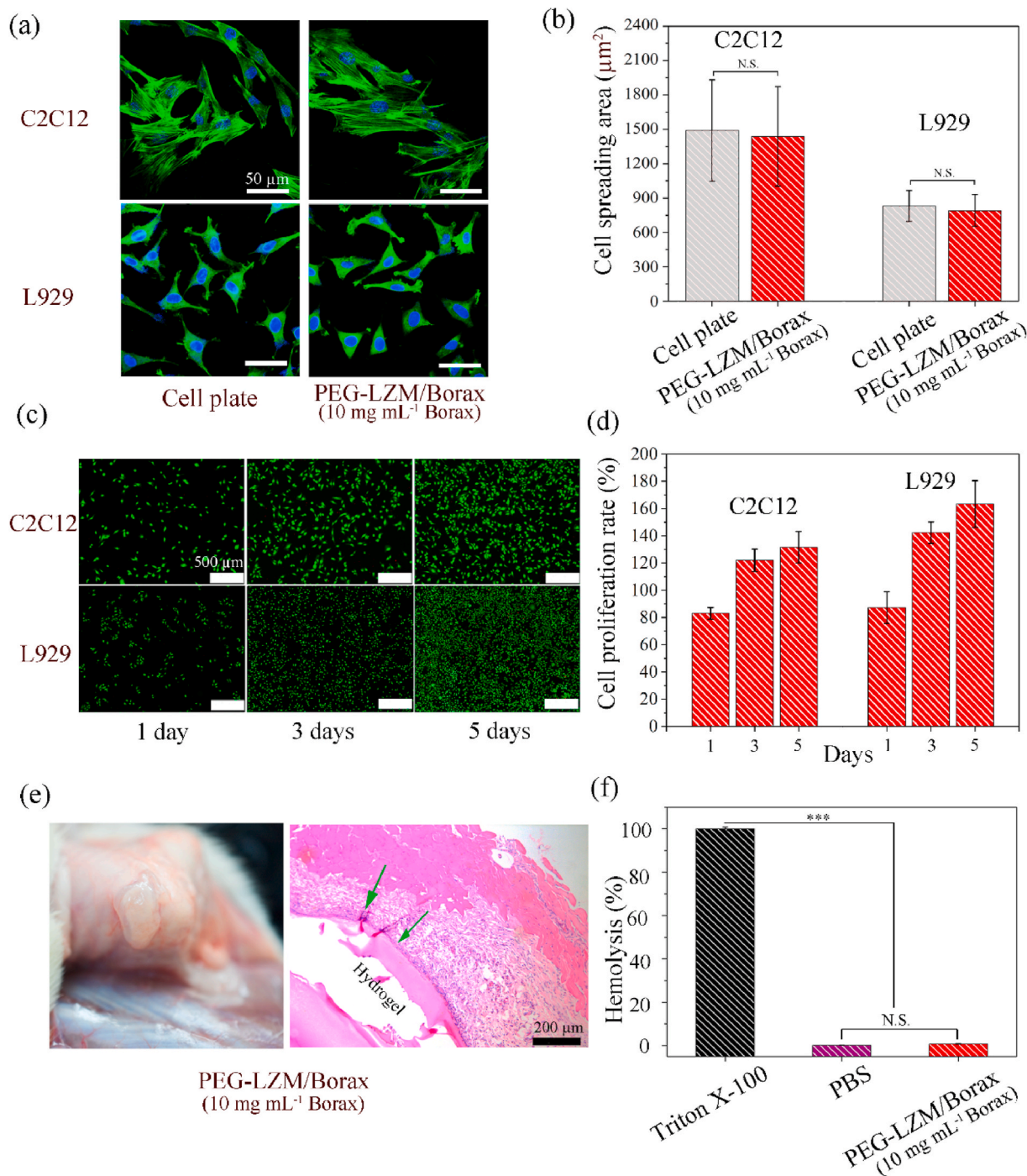


Fig. 6. Cell affinity and biocompatibility of PEG-LZM/Borax hydrogels. (a) Cell spreading morphology of C2C12 cells and L929 cells on the surface of a well plate and hydrogel (cytoskeleton fluorescence staining). (b) Average cell spreading area of different groups rely on immunofluorescence staining. (c) Live/dead immunofluorescence staining of cells seeded on the surface of PEG-LZM/Borax for different time. (d) Proliferation of cells seeded on PEG-LZM/Borax normalized to the cells seeding on the cell plate for 1 day. (e) In vivo biocompatibility of PEG-LZM/Borax hydrogel. (The photograph of the PEG-LZM/Borax hydrogel after implanting for 1 week, and the H&E staining of surrounding tissue) (f) The hemolytic ratio of different samples.

analysis results of wounds by H&E staining. The tissue around wound site in the control sample was accompanied with severe inflammatory cell infiltration indicated by the green arrow. In contrast, the inflammatory response was largely reduced in the group treated by PEG-LZM/Borax hydrogel. These results all indicate the PEG-LZM/Borax hydrogel also has good bactericidal abilities in vivo environment.

3.6. The hydrogel maintains its cell affinity and tissue/blood compatibility after borax addition

Our previous study has revealed that the PEG-LZM hydrogel can support cell growth through the RGD-like sequence on LZM, and it also has good tissue and blood compatibility, which may facilitate wound healing [8,53]. Since Borax has bactericidal ability, there is a concern that the presence of Borax may have a negative impact on its biological performance.

First, we evaluated the cell affinity of PEG-LZM/Borax hydrogel containing the highest content of borax (10 mg mL⁻¹ Borax) in this work. As shown in Fig. 6(a), immunofluorescent staining was performed to visualize the actin cytoskeleton and vinculin, respectively. The results indicate that actin networks of cells with significant outstretched filopodia extensions and lamellipodia protrusions (green) were observed in cells exposed to the PEG-LZM/Borax hydrogel, and no obvious morphological difference was observed compared with the cells on plate. Image J software was next used to calculate the spread area of cells on different matrix surfaces according to the fluorescence images of cells. Fig. 6(b) shows that the average spreading area of cells seeded on

the hydrogel was similar to that on the culture plate. The proliferation of cells exposed to the PEG-LZM/Borax hydrogel were examined by live/dead cell fluorescence staining (Fig. 6(c)) at different time scales, and almost no cell death was observed. Besides, the statistics results of proliferation are normalized to the cells seeding on the cell plate for 1 day by CCK-8 kit (Fig. 6(d)). The hydrogel mildly suppressed cell viability on the first day, and the cell viability of C2C12 and L929 was 83% and 89%, respectively. While a normal cell proliferation was observed for both C2C12 and L929 in the next 3 and 5 days. Therefore, these results indicate that the PEG-LZM/Borax hydrogel has a high cell affinity.

In order to assess the tissue compatibility of the PEG-LZM/Borax hydrogel (10 mg mL⁻¹ Borax), the hydrogel was injected in dorsal subcutaneous pockets of rats to observe the fibrosis and inflammation response. As observed in Fig. 6(e), no obvious fiber packages or intact collagen deposition were found on the surface of hydrogel after 1 week. H&E staining image also indicates only a little amount of inflammatory cells aggregated along the boundary of materials and tissue (green arrows), which may be due to a short-term normal immune response towards foreign materials. Blood compatibility was assayed by incubation PEG-LZM/Borax hydrogel (10 mg mL⁻¹ Borax) with blood red cells. The hemolytic ratio of hydrogel group was close to 0% (Fig. 6(f)), indicating the good blood compatibility of hydrogel.

These results all proved that the PEG-LZM hydrogel remains tissue/blood compatibility even containing a very high Borax amount.

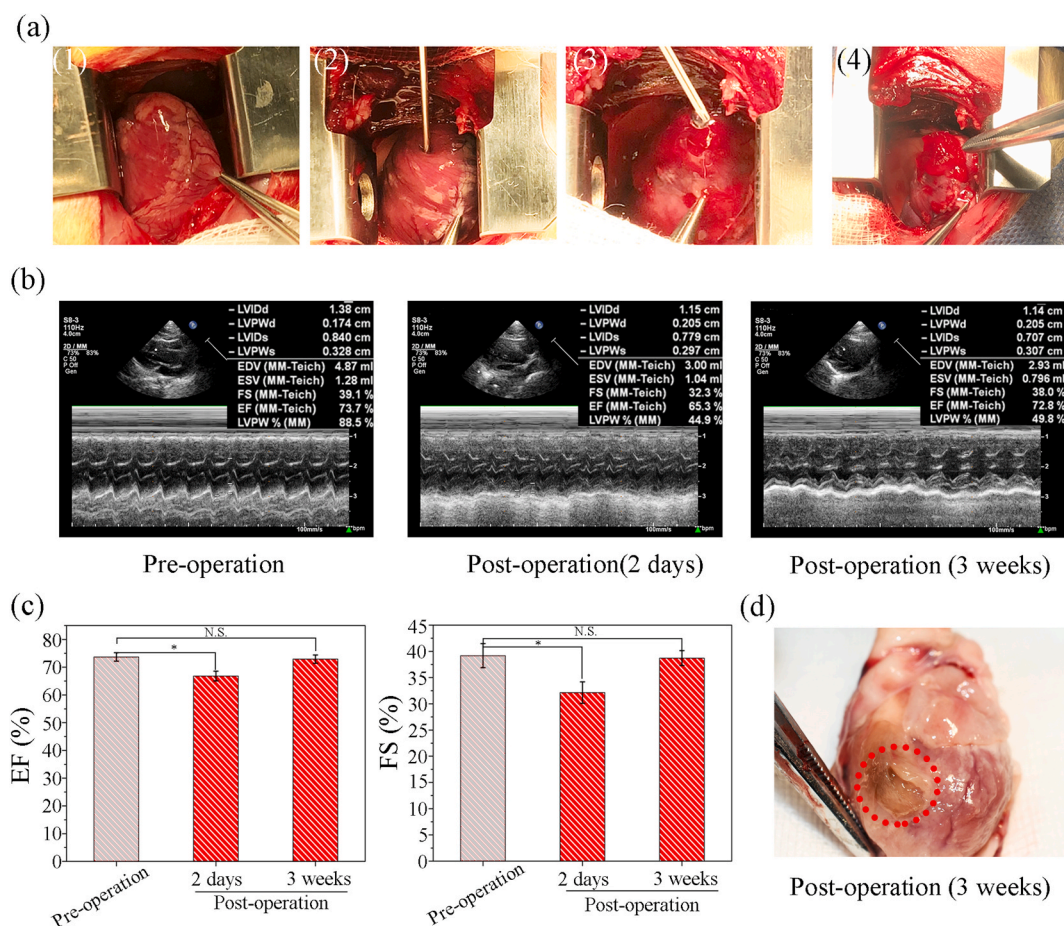


Fig. 7. PEG-LZM/Borax hydrogel with fastest gelation rate used for closure of left ventricular penetrating injury. (a) Operative process: (1) Exposure of left ventricle; (2) Establishment of a left ventricular penetrating injury by a 1.2 mm (inner diameter) needle; (3) Injecting hydrogel; (4) The wound was closed by spraying hydrogel. (b) Representative ECHO images for the normal heart before operation and the traumatic heart treated with hydrogel. (c) Statistical values of ejection fraction (EF %) and fractional shortening (FS %). (d) Photograph of myocardial wound at 3 weeks postoperatively.

3.7. In vivo modeling of tissue sealing

3.7.1. Rapid closure of left ventricular penetrating injury

As mentioned above, the gelation time of PEG-LZM hydrogel can be shortened to 3 s when containing 10 mg mL⁻¹ Borax, therefore such hydrogel has potential for rapidly closing bleeding wound in emergency.

To evaluate the performance of this hydrogel in vivo, a rabbit model with a transmural left ventricular (LV) wall defect (d: 1.2 mm) was established by puncture to mimic an emergent and bleeding injury. As shown in Fig. 7(a), the gelling precursor including 4-arm-PEG-NHS, LZM and Borax was injected to the wound site to close the defect and stop bleeding. Movie. S4 indicates a hydrogel formed rapidly in the presence of blood after being injected, which successfully closed the LV wall defect within few seconds. It is worth noting that the gel was directly applied to the LV wound without a purse-string suture assistance (i.e. a temporary wound closing technique in clinic to stop bleeding before wound treatment), compared with previous works [8,54]. Therefore, the Borax triggered instant hydrogel sealant appears to be more advantageous in emergency.

Supplementary video related to this article can be found at <https://doi.org/10.1016/j.bioactmat.2020.10.011>

The recovery of left ventricular functions was monitored by echocardiography (ECHO). After 2 days postoperatively, as displayed in Fig. 7(b) and (c), all the calculated ejection fraction (EF%) and shortened fraction (FS%) recovered to normal levels after 3 weeks postoperatively.

All the animals were sacrificed after ECHO measurement, and their wound sites were exposed for gross observation and histological evaluation. As shown in Fig. 7(d), the hydrogel was found to firmly adhere to the myocardial surface upon exposure to blood and a dynamic environment for 3 weeks (red circle). In addition, H&E staining (Fig. S7) shows a new connective tissue was generated at the original wound site, and no obvious inflammatory response and wound necrosis were seen around the wound.

These results prove that the borax-adjusted PEG-LZM hydrogel with rapid gelation rate can be used as a high-performance hemostasis in emergency.

3.7.2. Repair of gastric perforation

Many closed wounds such as gastric perforation, lung rupture, and liver injury, etc., represent a major threat to human life [55]. The adjustable gelation time of PEG-LZM/Borax provides convenience for

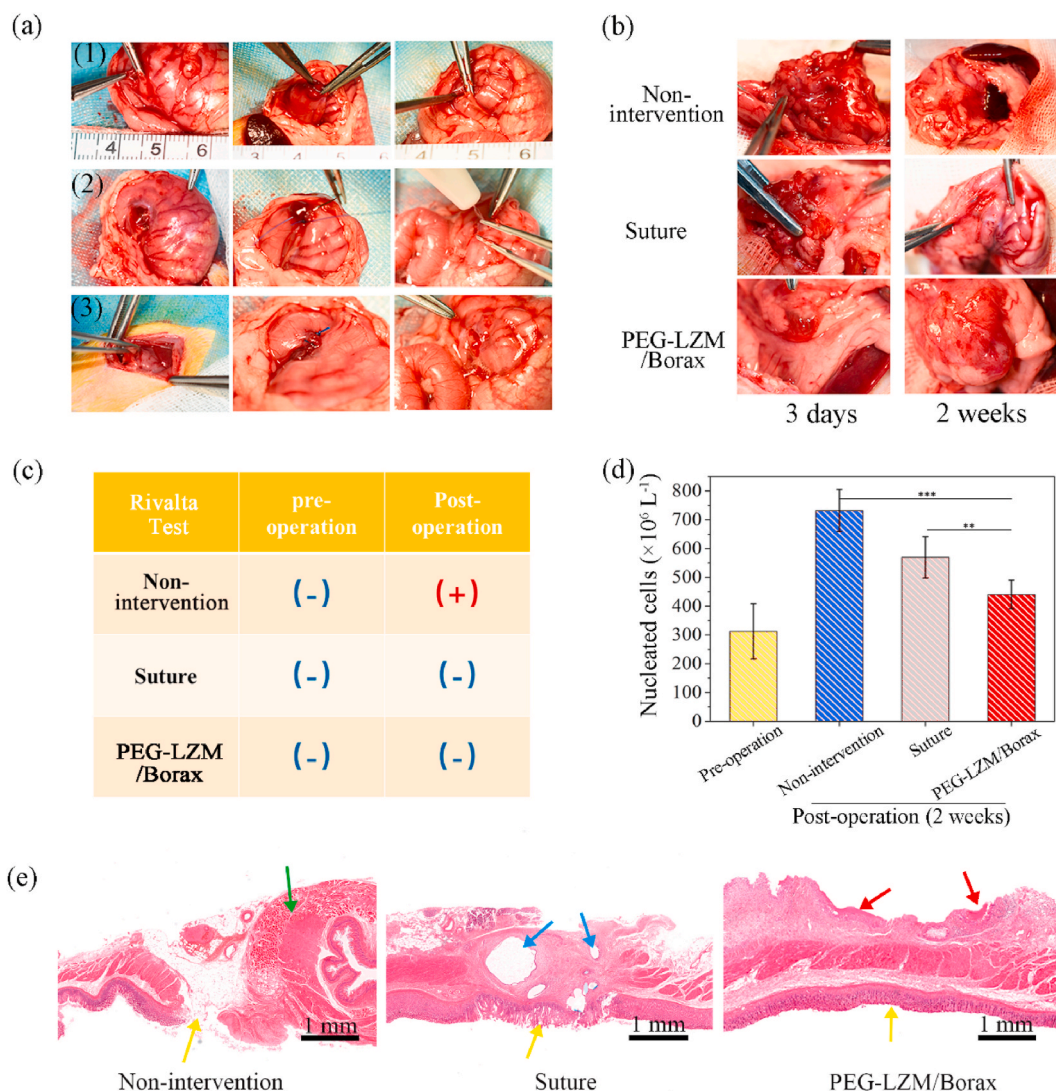


Fig. 8. PEG-LZM/Borax hydrogel used for repair of gastric perforation. (a) Operative process: (1) Establishment of a gastric perforation wound by a 2.0 mm (inner diameter) needle; (2) non-intervention (negative control), surgery Suture (positive control) or spraying PEG-LZM/Borax gelling solution; (3) Postoperative photographs of wounds. (b) Postoperative photographs of wounds for 3 days or 2 weeks. (c) Rivalta test and (d) nucleated cell density analysis of abdominal cleansing liquid before and after the operation (2 weeks). (e) Histological observation of wounds at 2 weeks postoperatively (H&E).

minimally invasive delivery of hydrogel for deep wounds treatment. Meanwhile, the presence of Borax is beneficial for ulcerative tissue recovery due to its drug properties [44]. However, because of the limitations of medical equipment used for animal experiments (such as gastroscopy, etc.), we cannot perform a real minimally invasive treatment of a rat gastric perforation model by using PEG-LZM/Borax. We here focused on evaluating the gel formation in situ for gastric perforation sealing and tissue recovery through an opening surgery.

Fig. 8(a) shows the experimental process. (1) A wound (d: 2 mm) on the rat stomach was established to mimic a gastric perforation. (2–3) PEG-LZM/Borax gelling solution was injected through a catheter to seal this defect, and non-intervention and wound suture were set as a negative and a positive control, respectively. Gastric wounds were checked after 3 days and 2 weeks postoperatively (Fig. 8(b)). The results show that the gastric juice and digestive food flowed out obviously from the stomach in the negative control group. In contrast, no obvious leakage of gastric contents was observed in the experimental group and the positive control group.

Rivalta assay is used to explore the inflammation in seroperitoneum. Positive (+) and negative (–) indicate that there is inflammatory effusion or not. As shown in Fig. 8(c), all the washing fluid of abdominal cavity were negative before surgery, while the negative control group turned positive in the non-intervention group, and the experimental group and positive group remained negative. At the same time, the number of nucleated cells in the different washing fluid were analyzed. Fig. 8(d) shows the number of nucleated cells in the hydrogel group was the lowest. These results demonstrate that the experimental group behaved the slightest inflammatory response.

After 2 weeks postoperatively, the repair effect of gastric wounds was evaluated by H&E staining. As observed in Fig. 8(e), the wound of non-intervention group was not closed as indicated by the yellow arrow, and some tissue adhesion occurred around the adventitia of the stomach (green arrow). In contrast, there was limited healing of the abdominal mucosa and submucosa at the wound in the group of sutures, and the muscle layer healing structure was disordered due to the space occupation of the suture (blue arrow). The abdominal mucosa and muscle layer of the stomach at the wound (yellow arrow) have been repaired completely after the intervention of PEG-LZM/Borax hydrogel (red arrow), and the tissue structure was clear, which may be due to abundant pharmacological activities of borax and the high cell affinity of lysozyme to promote tissue repairing.

These results all prove that the PEG-LZM/Borax hydrogel can be used as a high-performance sealant for the treatment of perforated injuries in the deep area of body.

3.8. In vivo wound healing evaluation

The wound healing performance of the PEG-LZM/Borax hydrogel (10 mg mL^{-1}) was further investigated in a full-thickness skin defect model. The photographs of postoperative wound healing in rats with different treatments at different time intervals were shown in Fig. S8(a), and the percentage of wound closure was displayed in Fig. S8(b). Throughout the wound healing process, hydrogel groups exhibited comparatively higher promotion effect than bare wound. On 14th day, the wound contraction of PEG-LZM/Borax and PEG-LZM was 91.8% and 92.8%, respectively, while the bare wound was only 86.8%, which demonstrated the better wound healing effect of PEG-LZM/Borax hydrogel.

4. Conclusion

In this work, the gelation time of an amidation reaction based hydrogel can be precisely regulated by a Chinese medicine Borax from seconds to minutes, because borax can buffer the pH of the gelation solution, which improves the nucleophilicity of $-\text{NH}_2$, thus promoting the gelation kinetics in a dose dependent manner. While the physical

properties of the adhesive remain constant.

The PEG-LZM/Borax hydrogel with the fastest gelation time ($\leq 3 \text{ s}$) can instantly close the LV wall defect to stop bleeding after injection. Furthermore, the precisely adjustable gelation time may also pave the way for the minimally invasive delivery of hydrogel for closed wound treatment. Ex vivo experiments prove that the gelation time of the PEG-LZM/Borax hydrogel can also be customized by Borax to match the required flowing time in the catheter. In vivo experiments indicate that such hydrogel can not only seal the defects, but also prevent bacterial infection and promote the wound repair, which may be due to the unique pharmacological activities of borax and the good cell affinity of the PEG-LZM hydrogel.

Based on the controllable gelation kinetic and versatile bioactivities, the PEG-LZM/Borax hydrogel represents a novel tissue adhesive for minimally invasive tissue/organ sealing or instant wound treatment. More broadly, our work provides a facile strategy for precisely regulation of gelation kinetics for other pH sensitive gelation system.

CRediT authorship contribution statement

Haoqi Tan: Conceptualization, Methodology, Writing - original draft. **Dawei Jin:** Conceptualization, Methodology, Writing - original draft. **Junjie Sun:** Investigation, Data curation. **Jialin Song:** Data curation. **Yao Lu:** Investigation. **Meng Yin:** Resources, Supervision, Validation. **Xin Chen:** Resources, Validation. **Xue Qu:** Supervision, Writing - review & editing. **Changsheng Liu:** Project administration.

Declaration of competing interest

The authors declare that they have no known competing financial interests or personal relationships that could have appeared to influence the work reported in this paper.

Acknowledgement

This work was supported by National Natural Science Foundation of China (grant number: 31922041, 51621002, 11932012 and 21875066), the science and technology innovation project of Shanghai Science and Technique Committee (18441908300), the Fundamental Research Funds for the Central Universities (SLD 00202006, JKVD12001032, JKVD12001002, 50321041916015).

Appendix A. Supplementary data

Supplementary data to this article can be found online at <https://doi.org/10.1016/j.bioactmat.2020.10.011>.

References

- [1] J.Q. Wang, F.J. Zhang, W.P. Tsang, C. Wan, C. Wu, Fabrication of injectable high strength hydrogel based on 4-arm star peg for cartilage tissue engineering, *Biomaterials* 120 (2017) 11–21.
- [2] Y.W. Lo, M.T. Sheu, W.H. Chiang, Y.L. Chiu, C.M. Tu, W.Y. Wang, M.H. Wu, Y. C. Wang, M. Lu, H.O. Ho, In situ chemically crosslinked injectable hydrogels for the subcutaneous delivery of trastuzumab to treat breast cancer, *Acta Biomater.* 86 (2019) 280–290.
- [3] S.S. Han, H.Y. Yoon, J.Y. Yhee, M.O. Cho, H.E. Shim, J.E. Jeong, D.E. Lee, K. Kim, H. Guim, J.H. Lee, K.M. Huh, S.W. Kang, In situ cross-linkable hyaluronic acid hydrogels using copper free click chemistry for cartilage tissue engineering, *Polym. Chem.* 9 (2018) 20–27.
- [4] R. Kelmansky, B.J. McAlvin, A. Nyska, J.C. Dohlman, H.H. Chiang, M. Hashimoto, D.S. Kohane, B. Mizrahi, Strong tissue glue with tunable elasticity, *Acta Biomater.* 53 (2017) 93–99.
- [5] Y.Z. Bu, L.C. Zhang, G.F. Sun, F.F. Sun, J.H. Liu, F. Yang, P.F. Tang, D.C. Wu, Tetrapeg based hydrogel sealants for in vivo visceral hemostasis, *Adv. Mater.* 31 (2019) 1901580.
- [6] Y.Z. Bu, L.C. Zhang, J.H. Liu, L.H. Zhang, T.T. Li, H. Shen, X. Wang, F. Yang, P. F. Tang, D.C. Wu, Synthesis and properties of hemostatic and bacteria-responsive in situ hydrogels for emergency treatment in critical situations, *ACS Appl. Mater. Interfaces* 8 (2016) 12674–12683.

- [7] R. Pinnarati, M.S.A. Bhuiyan, K. Meyers, R.M. Rajachar, B.P. Lee, Multifunctional biomedical adhesives, *Adv. Healthc. Mater.* 8 (2019) 1801568.
- [8] H.Q. Tan, D.W. Jin, X. Qu, H. Liu, X. Chen, M. Yin, C.S. Liu, A peg-lysozyme hydrogel harvests multiple functions as a fit-to-shape tissue sealant for internal-use of body, *Biomaterials* 192 (2019) 392–404.
- [9] S. Suzuki, Y. Ikada, *Biomaterials for Surgical Operation*, Humana Press, 2012.
- [10] F. Lee, J.E. Chung, M. Kurisawa, An injectable enzymatically crosslinked hyaluronic acid-tyramine hydrogel system with independent tuning of mechanical strength and gelation rate, *Soft Matter* 4 (2008) 880–887.
- [11] X.B. Ma, T.T. Xu, W. Chen, H.Y. Qin, B. Chi, Z.W. Ye, Injectable hydrogels based on the hyaluronic acid and poly (gamma-glutamic acid) for controlled protein delivery, *Carbohydr. Polym.* 179 (2018) 100–109.
- [12] P.Y. Sun, J. Wang, X. Yao, Y. Peng, X.X. Tu, P.F. Du, Z. Zheng, X.L. Wang, Facile preparation of mussel-inspired polyurethane hydrogel and its rapid curing behavior, *ACS Appl. Mater. Interfaces* 6 (2014) 12495–12504.
- [13] J. Li, F. Yu, G. Chen, J. Liu, X.L. Li, B. Cheng, X.M. Mo, C. Chen, J.F. Pan, Moist-retaining, self-recoverable, bioadhesive, and transparent in situ forming hydrogels to accelerate wound healing, *ACS Appl. Mater. Interfaces* 12 (2020) 2023–2038.
- [14] L.E. Jansen, L.J. Negron-Pineiro, S. Galarza, B.L. Peyton, Control of thiol-maleimide reaction kinetics in peg hydrogel networks, *Acta Biomater.* 70 (2018) 120–128.
- [15] Y.-H. Tsou, J. Khoneisser, P.-C. Huang, X. Xu, Hydrogel as a bioactive material to regulate stem cell fate, *Bioactive Materials* 1 (2016) 39–55.
- [16] O. Pinkas, D. Goder, R. Noyvirt, S. Peleg, M. Kahlon, M. Zilberman, Structuring of composite hydrogel bioadhesives and its effect on properties and bonding mechanism, *Acta Biomater.* 51 (2017) 125–137.
- [17] Y. Hong, F.F. Zhou, Y.J. Hua, X.Z. Zhang, C.Y. Ni, D.H. Pan, Y.Q. Zhang, D. M. Jiang, L. Yang, Q.N. Lin, Y.W. Zou, D.S. Yu, D.E. Arnot, X.H. Zou, L.Y. Zhu, S. F. Zhang, H.W. Ouyang, A strongly adhesive hemostatic hydrogel for the repair of arterial and heart bleeds, *Nat. Commun.* 10 (2019) 2060.
- [18] Y. Zhou, L. Gao, J. Peng, M. Xing, Y. Han, X. Wang, Y. Xu, J. Chang, Bioglass activated albumin hydrogels for wound healing, *Adv. Healthc. Mater.* 7 (2018) 1800144.
- [19] M. Patenaude, S. Campbell, D. Kinio, T. Hoare, Tuning gelation time and morphology of injectable hydrogels using ketone-hydrazide cross-linking, *Biomacromolecules* 15 (2014) 781–790.
- [20] A. Nishiguchi, Y. Kurihara, T. Taguchi, Underwater-adhesive microparticle dressing composed of hydrophobically-modified Alaska pollock gelatin for gastrointestinal tract wound healing, *Acta Biomater.* 99 (2019) 387–396.
- [21] T. Hayashi, T. Matsuyama, K. Hanada, K. Nakanishi, M. Uenoyama, M. Fujita, M. Ishihara, M. Kikuchi, T. Ikeda, H. Tajiri, Usefulness of photocrosslinkable chitosan for endoscopic cancer treatment in alimentary tract, *J. Biomed. Mater. Res. B* 71b (2004) 367–372.
- [22] A. Assmann, A. Vegh, M. Ghasemi-Rad, S. Bagherifard, G. Cheng, E.S. Sani, G. U. Ruiz-Esparza, I. Noshadi, A.D. Lassaletta, S. Gangadharan, A. Tamayol, A. Khademhosseini, N. Annabi, A highly adhesive and naturally derived sealant, *Biomaterials* 140 (2017) 115–127.
- [23] C.M. Elvin, T. Vuocolo, A.G. Brownlee, L. Sando, M.G. Huson, N.E. Liyow, P. R. Stockwell, R.E. Lyons, M. Kim, G.A. Edwards, G. Johnson, G.A. McFarland, J.A. M. Ramshaw, J.A. Werkmeister, A highly elastic tissue sealant based on photopolymerised gelatin, *Biomaterials* 31 (2010) 8323–8331.
- [24] E. Lih, J.S. Lee, K.M. Park, K.D. Park, Rapidly curable chitosan-peg hydrogels as tissue adhesives for hemostasis and wound healing, *Acta Biomater.* 8 (2012) 3261–3269.
- [25] Y.S. Li, X. Wang, Y.N. Fu, Y. Wei, L.Y. Zhao, L. Tao, Self-adapting hydrogel to improve the therapeutic effect in wound-healing, *ACS Appl. Mater. Interfaces* 10 (2018) 26046–26055.
- [26] L. Wang, F. Deng, W.W. Wang, A.F. Li, C.L. Lu, H. Chen, G. Wu, K.H. Nan, L.L. Li, Construction of injectable self-healing macroporous hydrogels via a template-free method for tissue engineering and drug delivery, *ACS Appl. Mater. Interfaces* 10 (2018) 36721–36732.
- [27] H.E. Davis, S.L. Miller, E.M. Case, J.K. Leach, Supplementation of fibrin gels with sodium chloride enhances physical properties and ensuing osteogenic response, *Acta Biomater.* 7 (2011) 691–699.
- [28] W. Chen, R. Wang, T.T. Xu, X.B. Ma, Z. Yao, B. Chi, H. Xu, A mussel-inspired poly (gamma-glutamic acid) tissue adhesive with high wet strength for wound closure, *J. Mater. Chem. B* 5 (2017) 5668–5678.
- [29] C.Y. Chang, A.T. Chan, P.A. Armstrong, H.C. Luo, T. Higuchi, I.A. Strehin, S. Vakrou, X.P. Lin, S.N. Brown, B. O'Rourke, T.P. Abraham, R.L. Wahl, C. J. Steenbergen, J.H. Elisseeff, M.R. Abraham, Hyaluronic acid-human blood hydrogels for stem cell transplantation, *Biomaterials* 33 (2012) 8026–8033.
- [30] S.F. Yan, W.D. Wang, X. Li, J. Ren, W.T. Yun, K.X. Zhang, G.F. Li, J.B. Yin, Preparation of mussel-inspired injectable hydrogels based on dual-functionalized alginate with improved adhesive, self-healing, and mechanical properties, *J. Mater. Chem. B* 6 (2018) 6377–6390.
- [31] B. Sarker, D.G. Papageorgiou, R. Silva, T. Zehnder, F. Gul-E-Noor, M. Bertmer, J. Kaschta, K. Chrissafis, R. Detsch, A.R. Boccaccini, Fabrication of alginate-gelatin crosslinked hydrogel microcapsules and evaluation of the microstructure and physico-chemical properties, *J. Mater. Chem. B* 2 (2014) 1470–1482.
- [32] Y.J. Zhong, J. Wang, Z.Y. Yuan, Y. Wang, Z.H. Xi, L. Li, Z.Y. Liu, X.H. Guo, A mussel-inspired carboxymethyl cellulose hydrogel with enhanced adhesiveness through enzymatic crosslinking, *Colloids Surf., B* 179 (2019) 462–469.
- [33] J. Qu, X. Zhao, P.X. Ma, B.L. Guo, Ph-responsive self-healing injectable hydrogel based on n-carboxyethyl chitosan for hepatocellular carcinoma therapy, *Acta Biomater.* 58 (2017) 168–180.
- [34] X.Q. Wang, B. Partlow, J. Liu, Z.Z. Zheng, B. Su, Y.S. Wang, D.L. Kaplan, Injectable silk-polyethylene glycol hydrogels, *Acta Biomater.* 12 (2015) 51–61.
- [35] D. Gyawali, P. Nair, H.K. Kim, J. Yang, Citrate-based biodegradable injectable hydrogel composites for orthopedic applications, *Biomater. Sci.* 1 (2013) 52–64.
- [36] M. Mehdizadeh, H. Weng, D. Gyawali, L.P. Tang, J. Yang, Injectable citrate-based mussel-inspired tissue bioadhesives with high wet strength for sutureless wound closure, *Biomaterials* 33 (2012) 7972–7983.
- [37] M. Shibayama, K. Nishi, T. Hiroi, Gelation kinetics and polymer network dynamics of homogeneous tetra-peg gels, *Macromol. Symp.* 348 (2015) 9–13.
- [38] B.M. Prentice, W.M. McGee, J.R. Stutzman, S.A. McLuckey, Strategies for the gas phase modification of cationized arginine via ion/ion reactions, *Int. J. Mass Spectrom.* 354 (2013) 211–218.
- [39] G. Pasut, F. Caboi, R. Schrepfer, G. Tonon, O. Schiavon, F.M. Veronese, New active poly(ethylene glycol) derivative for amino coupling, *React. Funct. Polym.* 67 (2007) 529–539.
- [40] M. Mentinova, N.Z. Barefoot, S.A. McLuckey, Solution versus gas-phase modification of peptide cations with nhs-ester reagents, *J. Am. Soc. Mass Spectrom.* 23 (2012) 282–289.
- [41] S. Madler, C. Bich, D. Touboul, R. Zenobi, Chemical cross-linking with nhs esters: a systematic study on amino acid reactivities, *J. Mass Spectrom.* 44 (2009) 694–706.
- [42] B. Balakrishnan, M. Mohanty, P.R. Umashankar, A. Jayakrishnan, Evaluation of an in situ forming hydrogel wound dressing based on oxidized alginate and gelatin, *Biomaterials* 26 (2005) 6335–6342.
- [43] B. Balakrishnan, M. Mohanty, A.C. Fernandez, P.V. Mohanan, A. Jayakrishnan, Evaluation of the effect of incorporation of dibutylryl cyclic adenosine monophosphate in an in situ-forming hydrogel wound dressing based on oxidized alginate and gelatin, *Biomaterials* 27 (2006) 1355–1361.
- [44] Y.K. Luo, M. Feng, Z.X. Fan, X.D. Zhu, F. Jin, R.Q. Li, J.B. Wu, X. Yang, Q.H. Jiang, H.F. Bai, Y.C. Huang, J.Y. Lang, Effect of kangfuxin solution on chemo/radiotherapy-induced mucositis in nasopharyngeal carcinoma patients: a multicenter, prospective randomized phase iii clinical study, *Evid. Based Complement, Alternative Med.* 2016 (2016) 8692343.
- [45] S.J. Gao, J.M. Guo, K. Nishinari, Thermoreversible konjac glucomannan gel crosslinked by borax, *Carbohydr. Polym.* 72 (2008) 315–325.
- [46] M. Shibayama, Y. Hiroiyuki, K. Hidenobu, F. Hiroshi, N. Shunji, Sol-gel transition of poly(vinyl alcohol)-borate complex, *Polymer* 29 (1988) 2066–2071.
- [47] M. Liang, J. Wang, M. Zhao, J. Cai, M. Zhang, N. Deng, B. Wang, B. Li, K. Zhang, Borax-assisted hydrothermal carbonization to fabricate monodisperse carbon spheres with high thermostability, *Mater. Res. Express* 6 (2019), 065615.
- [48] Y. Liu, H. Meng, S. Konst, R. Sarmiento, R. Rajachar, B.P. Lee, Injectable dopamine-modified poly(ethylene glycol) nanocomposite hydrogel with enhanced adhesive property and bioactivity, *ACS Appl. Mater. Interfaces* 6 (2014) 16982–16992.
- [49] C. Wei, W. Rui, X. Tingting, M. Xuebin, Y. Zhong, C. Bo, X. Hong, A mussel-inspired poly(c-glutamic acid) tissue adhesive with high wet strength for wound closure, *J. Mater. Chem. B* 5 (2017) 5668–5678.
- [50] M.T. Yilmaz, Minimum inhibitory and minimum bactericidal concentrations of boron compounds against several bacterial strains, *Turk. J. Med. Sci.* 42 (2012) 1423–1429.
- [51] X. Chen, S. Schauder, N. Potier, A. Van Dorsselaer, I. Pelczar, B.L. Bassler, F. M. Hughson, Structural identification of a bacterial quorum-sensing signal containing boron, *Nature* 415 (2002) 545–549.
- [52] C.A. Lowery, N.T. Salzedo, D. Sawada, G.F. Kaufmann, K.D. Janda, Medicinal chemistry as a conduit for the modulation of quorum sensing, *J. Med. Chem.* 53 (2010) 7467–7489.
- [53] N.P. Reynolds, M. Charnley, R. Mezzenga, P.G. Hartley, Engineered lysozyme amyloid fibril networks support cellular growth and spreading, *Biomacromolecules* 15 (2014) 599–608.
- [54] N. Lang, M.J. Pereira, Y. Lee, I. Friehs, N.V. Vasilyev, E.N. Feins, K. Ablasser, E. D. O'Ceirbhail, C. Xu, A. Fabozzo, R. Padera, S. Wasserman, F. Freudenthal, L. S. Ferreira, R. Langer, J.M. Karp, P.J. del Nido, A blood-resistant surgical glue for minimally invasive repair of vessels and heart defects, *Sci. Transl. Med.* 6 (2014) 218ra6.
- [55] K. Soreide, K. Thorsen, E.M. Harrison, J. Bingener, M.H. Moller, M. Ohene-Yeboah, J.A. Soreide, Perforated peptic ulcer, *Lancet* 386 (2015) 1288–1298.